Importance of counter-rotating coupling in the superfluid-to-Mott-insulator quantum phase transition of light in the Jaynes-Cummings lattice

Hang Zheng[1] and Yasutami Takada[2]
[1]*Key Laboratory of Artificial Structures and Quantum Control (Ministry of Education), Department of Physics, Shanghai Jiao Tong University, China*
[2]*Institute for Solid State Physics, The University of Tokyo, Kashiwa, Chiba 277-8581, Japan*
(Received 23 May 2011; published 11 October 2011)

The quantum phase transition between Mott insulator and superfluid is studied in the two-dimensional Jaynes-Cummings square lattice in which the counter-rotating coupling (CRC) is included. Both the ground state and the spectra of low-lying excitations are obtained with use of a sophisticated unitary transformation. This CRC is shown not only to induce a long-range interaction between cavities, favoring the long-range superfluid order, but also to break the conservation of local polariton number at each site, leading to the absence of the Mott lobes in the phase diagram, in sharp contrast with the case without the CRC as well as that of the Bose-Hubbard model.

DOI: 10.1103/PhysRevA.84.043819 PACS number(s): 42.50.Pq, 37.30.+i, 42.50.Ct, 05.30.Rt

I. INTRODUCTION

Quantum phase transitions and related phenomena constitute a field of great interest in the physics of strong correlation. In recent years, the Jaynes-Cummings lattice (JCL) attracts much attention in this field, partly because it is a very good model system for studying strongly correlated polariton physics and partly because it offers potential use of a quantum simulator for solid-state Hamiltonians, just like the cold-atom systems.

The JCL model is composed of a lattice of electromagnetic microcavities, each coupled to a two-level atom [1], and the intrasite Jaynes-Cummings (JC) coupling [2] is competed with the intersite photon hopping. A mean-field treatment of the model reveals a phase transition from Mott insulator to superfluid phase [3,4], resembling in large parts the phase diagram of the Bose-Hubbard model [5] with an eminent feature of the Mott lobes at the boundary between the insulating phase and the superfluid one. Both numerical [6–10] and analytical [3,4,11] methods have been employed to study the phase diagram as well as the spectra of low-lying excitations beyond the mean-field approximation and confirmed the existence of the Mott lobes.

All those theoretical studies, however, have not been done on the original JC model but under the rotating-wave approximation (RWA). To be specific, let us write the original Hamiltonian H for the JCL as

$$H = \sum_{\mathbf{l}} \left(H_{\mathbf{l}}^{\text{RWA}} + H_{\mathbf{l}}^{\text{CRC}} - \mu N_{\mathbf{l}}^{p} \right) - J \sum_{\langle \mathbf{l},\mathbf{l}' \rangle} b_{\mathbf{l}}^{\dagger} b_{\mathbf{l}'}, \qquad (1)$$

with $b_{\mathbf{l}}^{\dagger}$ ($b_{\mathbf{l}}$) the creation (annihilation) operator of cavity mode at site $\mathbf{l}$ with frequency ω, J the hopping strength between nearest-neighbor cavities $\mathbf{l}$ and $\mathbf{l}'$, and μ the chemical potential associated with $N_{\mathbf{l}}^{p}$ ($=\sigma_{\mathbf{l}}^{+}\sigma_{\mathbf{l}}^{-} + b_{\mathbf{l}}^{\dagger} b_{\mathbf{l}}$), the polariton number operator at site $\mathbf{l}$. The term $H_{\mathbf{l}}^{\text{RWA}}$ describes the JC model in the RWA as

$$H_{\mathbf{l}}^{\text{RWA}} = \epsilon \sigma_{\mathbf{l}}^{+}\sigma_{\mathbf{l}}^{-} + \omega b_{\mathbf{l}}^{\dagger} b_{\mathbf{l}} + g(b_{\mathbf{l}}^{\dagger}\sigma_{\mathbf{l}}^{-} + \sigma_{\mathbf{l}}^{+} b_{\mathbf{l}}), \qquad (2)$$

with $\sigma_{\mathbf{l}}^{\pm}$ the Pauli matrices representing the two-level-atom system characterized by the level difference ϵ and g the atom-photon coupling.

The counter-rotating coupling (CRC) term $H_{\mathbf{l}}^{\text{CRC}}$, neglected so far in the preceding works, is given by

$$H_{\mathbf{l}}^{\text{CRC}} = g(b_{\mathbf{l}}^{\dagger}\sigma_{\mathbf{l}}^{+} + \sigma_{\mathbf{l}}^{-} b_{\mathbf{l}}). \qquad (3)$$

It is true that this term contributes very little compared to the coupling terms in $H_{\mathbf{l}}^{\text{RWA}}$ in resonance experiments to detect real transitions, but virtual transitions contribute much to the formation of the ground state, making the RWA for the JCL model less reliable, especially for g of the order of ω and/or ϵ. Besides, the Mott lobes in the phase diagram may be considered as a consequence of the conservation of the local polariton number in the RWA, or $[H_{\mathbf{l}}^{\text{RWA}}, N_{\mathbf{l}}^{p}] = 0$, but the CRC breaks this conservation, i.e., $[H_{\mathbf{l}}^{\text{CRC}}, N_{\mathbf{l}}^{p}] \neq 0$, implying a radical change of the phase diagram, once the CRC is included. Moreover, the CRC induces an additional long-range interaction between cavities, enhancing a long-range ordering in the JCL model.

In view of this situation, we study the effect of the CRC on both Mott insulating and superfluid phases with use of a unitary transformation to eliminate the CRC term in H. We obtain a ground-state phase diagram as well as the spectra of low-lying excitations and find that *the Mott lobes are actually absent in the JCL model.*

II. UNITARY TRANSFORMATION

In the single-site JC problem, the ground state can be found rather trivially in the RWA, but it is not the case if the CRC is included. In order to overcome this difficulty, we perform a series of unitary transformations on H under the same guiding principles as described in Ref. [12] to obtain $H' = e^{S_2} e^{S_1} H e^{-S_1} e^{-S_2} = H_0' + H_1' + H_2'$, where S_1 is a displacement transformation

$$S_1 = \frac{1}{\sqrt{N}} \sum_{\mathbf{k}} \sum_{\mathbf{l}} \frac{g}{\omega_{\mathbf{k}}} \xi_{\mathbf{k}} \sigma_{\mathbf{l}}^{x} (b_{-\mathbf{k}}^{\dagger} - b_{\mathbf{k}}) e^{-i\mathbf{k}\cdot\mathbf{l}}, \qquad (4)$$

and S_2 is a squeezing transformation [13]

$$S_2 = \frac{1}{2} \sum_{\mathbf{k}} \ln(\tau_{\mathbf{k}})(b_{\mathbf{k}} b_{-\mathbf{k}} - b_{\mathbf{k}}^{\dagger} b_{-\mathbf{k}}^{\dagger}), \qquad (5)$$

where $b_{\mathbf{k}}$ is the Fourier transform of $b_{\mathbf{l}}$, N is the total number of cavities, $\omega_{\mathbf{k}} = \omega - \mu - zJ\gamma(\mathbf{k})$ (z the coordinate number), and $\gamma(\mathbf{k}) = [\cos(k_x) + \cos(k_y)]/2$ for a two-dimensional square lattice. The actual functional forms for the displacement $\xi_{\mathbf{k}}$ and the squeezing $\tau_{\mathbf{k}}$ will be given later.

The calculation along these transformations can be done straightforwardly to the end and the result is

$$H_0' = \frac{N}{2}\Delta - NV_0 + \frac{1}{4}\sum_{\mathbf{k}} \omega_{\mathbf{k}}\{\tau_{\mathbf{k}}^2(b_{-\mathbf{k}}^\dagger + b_{\mathbf{k}})^2 - \tau_{\mathbf{k}}^{-2}(b_{-\mathbf{k}}^\dagger - b_{\mathbf{k}})^2 - 2\} + \frac{1}{2}\sum_{\mathbf{l}} \eta\Delta\sigma_{\mathbf{l}}^z\left\{1 + \frac{1}{N}\sum_{\mathbf{k}}\frac{2g^2\xi_{\mathbf{k}}^2}{\omega_{\mathbf{k}}^2\tau_{\mathbf{k}}^2} \times (b_{\mathbf{k}}^\dagger b_{-\mathbf{k}}^\dagger + b_{\mathbf{k}}b_{-\mathbf{k}} - 2b_{\mathbf{k}}^\dagger b_{\mathbf{k}})\right\} - \frac{1}{N}\sum_{\mathbf{l},\mathbf{l}'}\sigma_{\mathbf{l}}^x\sigma_{\mathbf{l}'}^x\sum_{\mathbf{k}}\left\{\frac{g^2\xi_{\mathbf{k}}(2-\xi_{\mathbf{k}})}{\omega_{\mathbf{k}}} - V_0\right\}e^{i\mathbf{k}\cdot(\mathbf{l}-\mathbf{l}')}, \quad (6)$$

$$H_1' = \frac{1}{\sqrt{N}}\sum_{\mathbf{k}}\sum_{\mathbf{l}} g\tau_{\mathbf{k}}(1-\xi_{\mathbf{k}})\sigma_{\mathbf{l}}^x(b_{-\mathbf{k}}^\dagger + b_{\mathbf{k}})e^{-i\mathbf{k}\cdot\mathbf{l}} - \frac{1}{\sqrt{N}}\sum_{\mathbf{k}}\sum_{\mathbf{l}}\frac{g\eta\Delta}{\omega_{\mathbf{k}}\tau_{\mathbf{k}}}\xi_{\mathbf{k}} i\sigma_{\mathbf{l}}^y(b_{-\mathbf{k}}^\dagger - b_{\mathbf{k}})e^{-i\mathbf{k}\cdot\mathbf{l}}, \quad (7)$$

$$H_2' = \frac{\Delta}{2}\sum_{\mathbf{l}}\sigma_{\mathbf{l}}^z\left\{\cosh(X_{\mathbf{l}}) - \eta - \frac{1}{N} \times \sum_{\mathbf{k}}\frac{2\eta g^2\xi_{\mathbf{k}}^2}{\omega_{\mathbf{k}}^2\tau_{\mathbf{k}}^2}(b_{\mathbf{k}}^\dagger b_{-\mathbf{k}}^\dagger + b_{\mathbf{k}}b_{-\mathbf{k}} - 2b_{\mathbf{k}}^\dagger b_{\mathbf{k}})\right\} - \frac{\Delta}{2}\sum_{\mathbf{l}} i\sigma_{\mathbf{l}}^y\{\sinh(X_{\mathbf{l}}) - \eta X_{\mathbf{l}}\}, \quad (8)$$

where the parameters Δ and η are defined as

$$\Delta = \epsilon - \mu \text{ and } \eta = \exp\left(-\frac{2}{N}\sum_{\mathbf{k}}\frac{g^2\xi_{\mathbf{k}}^2}{\omega_{\mathbf{k}}^2\tau_{\mathbf{k}}^2}\right), \quad (9)$$

respectively, and the operator $X_{\mathbf{l}}$ is introduced as

$$X_{\mathbf{l}} = \frac{2}{\sqrt{N}}\sum_{\mathbf{k}}\frac{g\xi_{\mathbf{k}}}{\omega_{\mathbf{k}}\tau_{\mathbf{k}}}e^{-i\mathbf{k}\cdot\mathbf{l}}(b_{-\mathbf{k}}^\dagger - b_{\mathbf{k}}). \quad (10)$$

The last term in H_0' is an induced long-range Ising-type interaction between atoms in different cavities, in which V_0, defined as

$$V_0 = \frac{1}{N}\sum_{\mathbf{k}}\frac{g^2}{\omega_{\mathbf{k}}}\xi_{\mathbf{k}}(2-\xi_{\mathbf{k}}), \quad (11)$$

is subtracted so as to eliminate a constant self-interaction at the same site.

The terms in proportion to η in H_0' and H_1' are exactly canceled by the corresponding ones in H_2', but it is very important to define H_2' in the present form of Eq. (8), as we shall explain in the following: Basically, the "photon-dressing" parameter η arises from the rearrangement of the operator $\exp(X_{\mathbf{l}})$ into the form of normal ordering with respect to the photon operators:

$$\exp(X_{\mathbf{l}}) = \eta\exp\left(\frac{2}{\sqrt{N}}\sum_{\mathbf{k}}\lambda_{\mathbf{k}}e^{-i\mathbf{k}\cdot\mathbf{l}}b_{-\mathbf{k}}^\dagger\right) \times \exp\left(-\frac{2}{\sqrt{N}}\sum_{\mathbf{k}}\lambda_{\mathbf{k}}e^{-i\mathbf{k}\cdot\mathbf{l}}b_{\mathbf{k}}\right), \quad (12)$$

where $\lambda_{\mathbf{k}} = g\xi_{\mathbf{k}}/\omega_{\mathbf{k}}\tau_{\mathbf{k}}$. Then, it is easy to see that $\sinh(X_{\mathbf{l}}) - \eta X_{\mathbf{l}}$ in the second term in H_2' consists of the products of at least three photon operators in normal ordering. (Needless to say, this photon operator is not a bare one, but an effective one renormalized by the unitary transformations.) On the other hand, the dominant contribution to the first term in H_2' is proportional to the operator

$$\sum_{\mathbf{l}}\left\{\cosh(X_{\mathbf{l}}) - \eta - \frac{2\eta}{N} \times \sum_{\mathbf{k}}\lambda_{\mathbf{k}}^2(b_{\mathbf{k}}^\dagger b_{-\mathbf{k}}^\dagger + b_{\mathbf{k}}b_{-\mathbf{k}} - 2b_{\mathbf{k}}^\dagger b_{\mathbf{k}})\right\}$$

because $\sigma_{\mathbf{l}}^z$ is well approximated to be -1, a constant independent of site index $\mathbf{l}$, as we shall see in the linearized spin-wave approximation. Then, the predominant contribution originates from the products of at least four photon operators in normal ordering.

As a result, one can see that the dominant parts of H_2' in the form of Eq. (8) are composed of terms of three, or a higher number of, photon operators, which enables us to drop H_2' hereafter. Note, however, that this neglect of H_2' does not mean that our calculation is valid only up to second order in g; it is a well-known fact in the physics of polarons and bipolarons that the strong-coupling effects on the ground and low-lying excited states can be included to a satisfactory degree up to infinite order of g in terms of the photon-dressing parameter η. Therefore, as long as we employ H_0' and H_1' in the forms of Eqs. (6) and (7), respectively, with using η in Eq. (9), we believe that our calculation scheme of neglecting H_2' will work very well even for the strong-coupling region of g.

For the substantiation of our belief, we have assessed the accuracy of our scheme by checking the single- and double-site JC model. (Details are given in Appendices A and B.) In Fig. 1, we have favorably compared our results for the ground-state energy E_g of the single-site JC model [Eq. (A6)] with the exact ones obtained numerically by exact diagonalization of H in Eq. (1) for the single-site case. We have also obtained satisfactory agreement between our results for n as the ground-state-average polariton number per site [Eq. (A10)] with those in the exact calculation. In addition to such numerical calculations, we have also calculated the perturbation contribution of H_2' to the ground-state properties for the single-site JC model in Appendix A and have found that it is less than 2%, even for the resonant and moderately strong coupling case of $\omega = \epsilon = g$.

Similar comparison is made in Fig. 2 for the double-site JC model to confirm enough accuracy of our calculation scheme in the weak-hopping region. It must be noted here that the level crossover, which is predicted to occur in the RWA and constitutes an important ingredient for the emergence of the Mott lobes, is eliminated by the CRC. Concomitantly, the

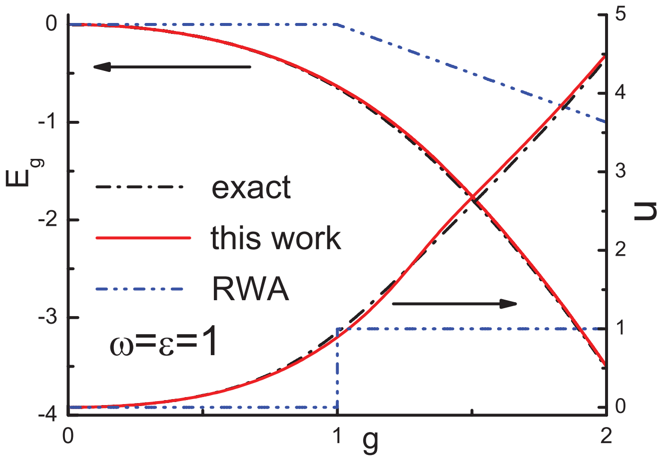

FIG. 1. (Color online) Approximate results in our scheme (solid curves) as well as those in the RWA (double dotted-dashed lines) for the ground-state energy E_g and the ground-state-average polariton number per site n are compared with the corresponding exact ones (dotted-dashed curves) for the single-site JC model at the resonant condition $\epsilon = \omega$. Energies are in units of ω.

ground-state polariton number changes continuously in both the exact and our approximate results, in sharp contrast with the jump in the excitation number found in the RWA.

In order to estimate the degradation of our approximation scheme with the increase of J, the hopping parameter between two cavities, we plot the results of both E_g and n as a function of J/g for the double-site JC model at $\epsilon = g = \omega$. One can see that, although the RWA always gives poor results, our approach provides satisfactory results for E_g and reasonably good estimates for n, even if J is increased by an order of magnitude from the case in Fig. 2. Thus, we are confident of the accuracy of our scheme.

III. INSULATING PHASE

The Pauli matrices in H' ($\approx H_0' + H_1'$), $\sigma_{\mathbf{l}}^{z,\pm}$ may be treated by the linearized spin-wave approximation [14] as

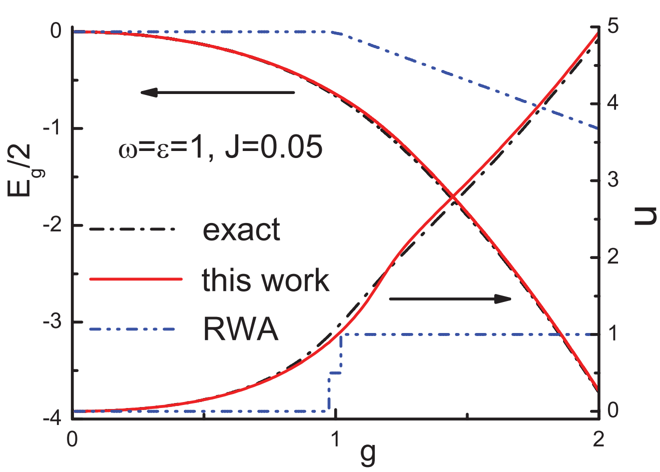

FIG. 2. (Color online) Comparison similar to that in Fig. 1 is made for the double-site JC model at $\epsilon = \omega$ and $J = 0.05\omega$ (the weak-hopping case). Energies are in units of ω.

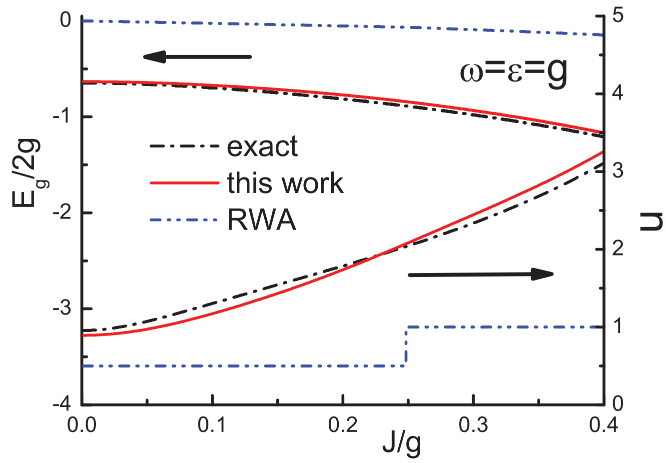

FIG. 3. (Color online) Similar comparison is made as a function of J/g for the double-site JC model at $\epsilon = g = \omega$. Energies are in units of ω.

$\sigma_{\mathbf{l}}^z = 2a_{\mathbf{l}}^\dagger a_{\mathbf{l}} - 1$, $\sigma_{\mathbf{l}}^+ = a_{\mathbf{l}}^\dagger$, and $\sigma_{\mathbf{l}}^- = a_{\mathbf{l}}$ with $a_{\mathbf{l}}$ and $a_{\mathbf{l}}^\dagger$ bosonic operators. Then, H' is approximated as

$$\begin{aligned} H' \approx H^I = {} & \frac{1-\eta}{2}\Delta N - NV_0 + \frac{1}{4}\sum_{\mathbf{k}}\omega_{\mathbf{k}}\left(\tau_{\mathbf{k}}^2 + \tau_{\mathbf{k}}^{-2} - 2\right) \\ & + \sum_{\mathbf{k}}\omega_{\mathbf{k}}\tau_{\mathbf{k}}^2 b_{\mathbf{k}}^\dagger b_{\mathbf{k}} + \sum_{\mathbf{k}}\eta\Delta a_{\mathbf{k}}^\dagger a_{\mathbf{k}} \\ & - \sum_{\mathbf{k}}\left\{\frac{g^2}{\omega_{\mathbf{k}}}\xi_{\mathbf{k}}(2-\xi_{\mathbf{k}}) - V_0\right\}(a_{-\mathbf{k}}^\dagger + a_{\mathbf{k}})(a_{\mathbf{k}}^\dagger + a_{-\mathbf{k}}) \\ & + \sum_{\mathbf{k}} g\tau_{\mathbf{k}}(1-\xi_{\mathbf{k}})(b_{-\mathbf{k}}^\dagger + b_{\mathbf{k}})(a_{\mathbf{k}}^\dagger + a_{-\mathbf{k}}) \\ & - \sum_{\mathbf{k}}\frac{g\eta\Delta}{\omega_{\mathbf{k}}\tau_{\mathbf{k}}}\xi_{\mathbf{k}}(b_{-\mathbf{k}}^\dagger - b_{\mathbf{k}})(a_{\mathbf{k}}^\dagger - a_{-\mathbf{k}}), \end{aligned} \tag{13}$$

where $a_{\mathbf{k}}$ is the running-wave operator of $a_{\mathbf{l}}$ and $\tau_{\mathbf{k}}$ is the squeezing function, given by

$$\tau_{\mathbf{k}}^2 = \sqrt{1 + 4\eta\Delta g^2\xi_{\mathbf{k}}^2/\omega_{\mathbf{k}}^3}. \tag{14}$$

In Eq. (13), we have kept only the quadratic operator terms, neglecting all cubic and quartic terms so as to focus on the ground and low-lying excited states.

We further apply a Bogoliubov transformation to H^I as

$$\begin{aligned} e^{S_3}H^I e^{-S_3} = {} & E_g^I + \sum_{\mathbf{k}}\omega_{\mathbf{k}}\tau_{\mathbf{k}}^2 b_{\mathbf{k}}^\dagger b_{\mathbf{k}} + \sum_{\mathbf{k}}\eta\Delta\rho_{\mathbf{k}}^2 a_{\mathbf{k}}^\dagger a_{\mathbf{k}} \\ & + \sum_{\mathbf{k}}\tilde{g}_{I\mathbf{k}}(b_{\mathbf{k}}^\dagger a_{\mathbf{k}} + a_{\mathbf{k}}^\dagger b_{\mathbf{k}}), \end{aligned} \tag{15}$$

with

$$S_3 = \frac{1}{2}\sum_{\mathbf{k}}\ln(\rho_{\mathbf{k}})(a_{\mathbf{k}}^\dagger a_{-\mathbf{k}}^\dagger - a_{\mathbf{k}}a_{-\mathbf{k}}), \tag{16}$$

where $\tilde{g}_{I\mathbf{k}} = 2g\tau_{\mathbf{k}}(1-\xi_{\mathbf{k}})/\rho_{\mathbf{k}}$, with $\rho_{\mathbf{k}}$ and $\xi_{\mathbf{k}}$ given by

$$\rho_{\mathbf{k}}^2 = \sqrt{1 - 4[g^2\xi_{\mathbf{k}}(2-\xi_{\mathbf{k}})/\omega_{\mathbf{k}} - V_0]/\eta\Delta}, \tag{17}$$

$$\xi_{\mathbf{k}} = \omega_{\mathbf{k}}\tau_{\mathbf{k}}^2/\left(\omega_{\mathbf{k}}\tau_{\mathbf{k}}^2 + \eta\Delta\rho_{\mathbf{k}}^2\right). \tag{18}$$

The ground-state energy of the insulating phase is obtained as

$$E_g^I = \frac{1}{2}N(1-2\eta)\Delta - NV_0 + \frac{1}{4}\sum_{\mathbf{k}}\omega_{\mathbf{k}}\left(\tau_{\mathbf{k}}^2+\tau_{\mathbf{k}}^{-2}-2\right)+\frac{1}{2}\eta\Delta\sum_{\mathbf{k}}\rho_{\mathbf{k}}^2. \quad (19)$$

Note that, because of the choice of $\xi_{\mathbf{k}}$ and $\tau_{\mathbf{k}}^2$, $e^{S_3}H^I e^{-S_3}$ is of the form of rotating-wave coupling between $a_{\mathbf{k}}$ and $b_{\mathbf{k}}$, allowing us to write the ground state of the form of $|G_I\rangle = |\{a_{\mathbf{k}}^\dagger a_{\mathbf{k}}=0\}\rangle|\{b_{\mathbf{k}}^\dagger b_{\mathbf{k}}=0\}\rangle$.

Diagonalization of H^I determines the excitation energies of two branches $E_I^{\pm}(\mathbf{k})$ in the insulating phase as

$$E_I^{\pm}(\mathbf{k}) = \tfrac{1}{2}\left(\eta\Delta\rho_{\mathbf{k}}^2+\omega_{\mathbf{k}}\tau_{\mathbf{k}}^2\right) \pm \tfrac{1}{2}\sqrt{\left(\eta\Delta\rho_{\mathbf{k}}^2-\omega_{\mathbf{k}}\tau_{\mathbf{k}}^2\right)^2+4\tilde{g}_{I\mathbf{k}}^2}. \quad (20)$$

In Fig. 4, the lower branch $E_I^-(\mathbf{k})$ is plotted for the resonant case of $\omega=\epsilon$ and $\Delta/g=1.1$. In the weak-hopping situation, there exists a gap at $\mathbf{k}=0$ in the excitation spectrum, as can be seen at $zJ/g=0.08$, but the gap disappears at $zJ/g = 0.088\,76$, and for $zJ/g > 0.088\,76$, $E_I^-(\mathbf{0})$ becomes negative, indicating that the insulating phase is no longer stable for this situation, suggesting that the superfluid phase should occur instead. Thus, the condition for the presence of the stable insulating phase may be written as

$$\eta\Delta\rho_{\mathbf{0}}^2\omega_{\mathbf{0}}\tau_{\mathbf{0}}^2 \geqslant \tilde{g}_{I\mathbf{0}}^2 \Rightarrow 2G_0 \leqslant \eta\Delta, \quad (21)$$

where $G_0 = 2(g^2/\omega_{\mathbf{0}} - V_0)$.

This condition can be used to determine the phase boundary between the insulating and the superfluid phases, and the result is shown in Fig. 5. For comparison, the Mott lobes predicted in the RWA are also plotted to show that we have obtained a totally different phase boundary.

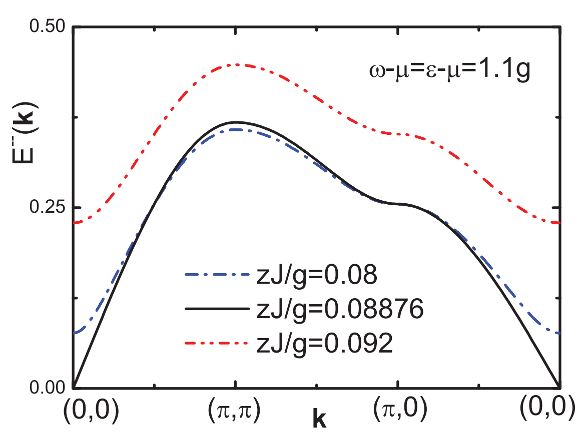

FIG. 4. (Color online) Dispersion relation of the lower-branch excitation for the two-dimensional JC square lattice at $\omega=\epsilon$ and $\Delta/g=1.1$. Energies are in units of ω. The excitation energies are gapped in both insulating ($zJ/g=0.08$) and superfluid ($zJ/g = 0.092$) phases except for the case of $zJ/g = 0.088\,76$, at which the phase transition occurs.

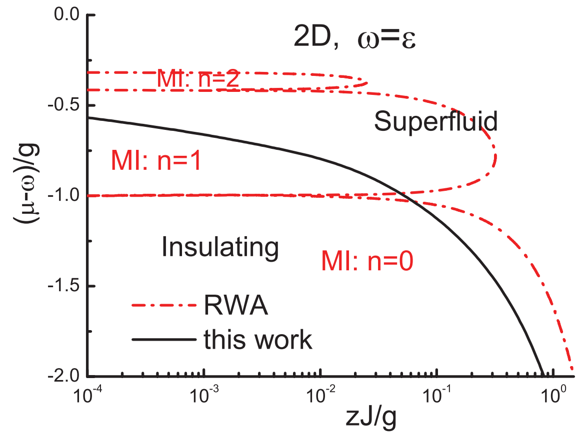

FIG. 5. (Color online) Phase diagram in $(zJ/g,(\mu-\omega)/g)$ space for the two-dimensional JC square lattice at the resonant condition $\omega=\epsilon$.

IV. SUPERFLUID PHASE

In the superfluid phase with $2G_0 > \eta\Delta$, we introduce a static displacement of the $\mathbf{k}=0$ photon mode to transform H_0' and H_1' as

$$\begin{aligned} e^R H_0' e^{-R} =& \frac{N\Delta}{2} - NV_0 + \frac{NG_0\sigma_0^2}{2} \\ &+ \frac{1}{4}\sum_{\mathbf{k}}\omega_{\mathbf{k}}\left\{\tau_{\mathbf{k}}^2(b_{-\mathbf{k}}^\dagger+b_{\mathbf{k}})^2-\tau_{\mathbf{k}}^{-2}(b_{-\mathbf{k}}^\dagger-b_{\mathbf{k}})^2-2\right\} \\ &+ \frac{1}{N}\sum_{\mathbf{k}}\frac{g^2\xi_{\mathbf{k}}^2}{\omega_{\mathbf{k}}^2\tau_{\mathbf{k}}^2}\left(b_{\mathbf{k}}^\dagger b_{-\mathbf{k}}^\dagger + b_{\mathbf{k}}b_{-\mathbf{k}} - 2b_{\mathbf{k}}^\dagger b_{\mathbf{k}}\right) \\ &\times \sum_{\mathbf{l}}\eta\Delta\sigma_{\mathbf{l}}^z + \frac{1}{2}\sum_{\mathbf{l}}\eta\Delta\sigma_{\mathbf{l}}^z - \sum_{\mathbf{l}}G_0\sigma_0\sigma_{\mathbf{l}}^x \\ &- \frac{1}{N}\sum_{\mathbf{k}}\left(\frac{g^2\xi_{\mathbf{k}}(2-\xi_{\mathbf{k}})}{\omega_{\mathbf{k}}} - V_0\right) \\ &\times \sum_{\mathbf{i},\mathbf{j}} e^{i\mathbf{k}\cdot(\mathbf{i}-\mathbf{j})}(\sigma_{\mathbf{i}}^x-\sigma_0)(\sigma_{\mathbf{j}}^x-\sigma_0), \end{aligned} \quad (22)$$

$$\begin{aligned} e^R H_1' e^{-R} =& \frac{1}{\sqrt{N}}\sum_{\mathbf{k}} g\tau_{\mathbf{k}}(1-\xi_{\mathbf{k}})(b_{-\mathbf{k}}^\dagger+b_{\mathbf{k}}) \\ &\times \sum_{\mathbf{l}} e^{-i\mathbf{k}\cdot\mathbf{l}}(\sigma_{\mathbf{l}}^x-\sigma_0) - \frac{1}{\sqrt{N}}\sum_{\mathbf{k}}\frac{g\eta\Delta}{\omega_{\mathbf{k}}\tau_{\mathbf{k}}} \\ &\times \xi_{\mathbf{k}}(b_{-\mathbf{k}}^\dagger - b_{\mathbf{k}})\sum_{\mathbf{l}} i\sigma_{\mathbf{l}}^y e^{-i\mathbf{k}\cdot\mathbf{l}}, \end{aligned} \quad (23)$$

with the operator R defined by

$$R = \sqrt{N}g\sigma_0(1-\xi_{\mathbf{0}})(b_{\mathbf{0}}^\dagger - b_{\mathbf{0}})/\omega_{\mathbf{0}}\tau_{\mathbf{0}}. \quad (24)$$

The subscript $\mathbf{0}$ in Eq. (24) refers to the case of $\mathbf{k}=0$. Then, after a rotation of the Pauli matrices at every site $\mathbf{l}$ as

$$H'' = U^\dagger e^R(H_0'+H_1')e^{-R}U = H_0''+H_1'', \quad (25)$$

with a unitary matrix U given by

$$U = \prod_{\mathbf{l}}\left(v\sigma_{\mathbf{l}}^x - u\sigma_{\mathbf{l}}^z\right), \quad (26)$$

where the parameters u and v are, respectively, determined as $u = \sqrt{(1+\eta\Delta/W)/2}$ and $v = \sqrt{(1-\eta\Delta/W)/2}$ with $W = \sqrt{4G_0^2\sigma_0^2 + \eta^2\Delta^2}$ and $\sigma_0^2 = 1 - \eta^2\Delta^2/4G_0^2$, we get the expressions for H_0'' and H_1'' as

$$\begin{aligned} H_0'' = {} & \frac{N\Delta}{2} - NV_0 + \frac{NG_0\sigma_0^2}{2} + \frac{1}{4}\sum_{\mathbf{k}} \omega_{\mathbf{k}}\left\{\tau_{\mathbf{k}}^2(b_{-\mathbf{k}}^\dagger + b_{\mathbf{k}})^2 - \tau_{\mathbf{k}}^{-2}(b_{-\mathbf{k}}^\dagger - b_{\mathbf{k}})^2 - 2\right\} \\ & + \frac{1}{N}\sum_{\mathbf{k}} \frac{g^2\xi_{\mathbf{k}}^2}{\omega_{\mathbf{k}}^2\tau_{\mathbf{k}}^2}(b_{\mathbf{k}}^\dagger b_{-\mathbf{k}}^\dagger + b_{\mathbf{k}}b_{-\mathbf{k}} - 2b_{\mathbf{k}}^\dagger b_{\mathbf{k}})\sum_{\mathbf{l}} \eta\Delta\left(\frac{\eta\Delta}{W}\sigma_{\mathbf{l}}^z - \sigma_0\sigma_{\mathbf{l}}^x\right) + \frac{1}{2}\sum_{\mathbf{l}} W\sigma_{\mathbf{l}}^z \\ & - \frac{1}{N}\sum_{\mathbf{k}}\left\{\frac{g^2\xi_{\mathbf{k}}(2-\xi_{\mathbf{k}})}{\omega_{\mathbf{k}}} - V_0\right\}\sum_{\mathbf{i},\mathbf{j}} e^{i\mathbf{k}\cdot(\mathbf{i}-\mathbf{j})}\left\{\frac{\eta\Delta}{W}\sigma_{\mathbf{i}}^x + \sigma_0\left(\sigma_{\mathbf{i}}^z + 1\right)\right\}\left\{\frac{\eta\Delta}{W}\sigma_{\mathbf{j}}^x + \sigma_0\left(\sigma_{\mathbf{j}}^z + 1\right)\right\}, \end{aligned} \tag{27}$$

$$H_1'' = \frac{1}{\sqrt{N}}\sum_{\mathbf{k}} \frac{g\eta\Delta}{\omega_{\mathbf{k}}\tau_{\mathbf{k}}}\xi_{\mathbf{k}}(b_{-\mathbf{k}}^\dagger - b_{\mathbf{k}})\sum_{\mathbf{l}} i\sigma_{\mathbf{l}}^y e^{-i\mathbf{k}\cdot\mathbf{l}} - \frac{1}{\sqrt{N}}\sum_{\mathbf{k}} g\tau_{\mathbf{k}}(1-\xi_{\mathbf{k}})(b_{-\mathbf{k}}^\dagger + b_{\mathbf{k}})\sum_{\mathbf{l}} e^{-i\mathbf{k}\cdot\mathbf{l}}\left\{\frac{\eta\Delta}{W}\sigma_{\mathbf{l}}^x + \sigma_0\left(\sigma_{\mathbf{l}}^z + 1\right)\right\}. \tag{28}$$

The linearized spin-wave approximation, together with the same approximation as used in deriving Eq. (13), is further employed in H'' to reach H^S as

$$\begin{aligned} H'' \approx H^S = {} & \frac{1}{2}N(\Delta - W) - NV_0 + \frac{NG_0\sigma_0^2}{2} + \frac{1}{4}\sum_{\mathbf{k}}\omega_{\mathbf{k}}\left(\tau_{\mathbf{k}}^2 + \tau_{\mathbf{k}}^{-2} - 2\right) \\ & + \sum_{\mathbf{k}}\omega_{\mathbf{k}}\tau_{\mathbf{k}}^2 b_{\mathbf{k}}^\dagger b_{\mathbf{k}} + \sum_{\mathbf{k}} W a_{\mathbf{k}}^\dagger a_{\mathbf{k}} - \left(\frac{\eta\Delta}{W}\right)^2\sum_{\mathbf{k}}\left\{\frac{g^2\xi_{\mathbf{k}}(2-\xi_{\mathbf{k}})}{\omega_{\mathbf{k}}} - V_0\right\}(a_{-\mathbf{k}}^\dagger + a_{\mathbf{k}})(a_{\mathbf{k}}^\dagger + a_{-\mathbf{k}}) \\ & + \sum_{\mathbf{k}}\frac{g\eta\Delta}{\omega_{\mathbf{k}}\tau_{\mathbf{k}}}\xi_{\mathbf{k}}(b_{-\mathbf{k}}^\dagger - b_{\mathbf{k}})(a_{\mathbf{k}}^\dagger - a_{-\mathbf{k}}) - \sum_{\mathbf{k}}\frac{g\eta\Delta}{W}\tau_{\mathbf{k}}(1-\xi_{\mathbf{k}})(b_{-\mathbf{k}}^\dagger + b_{\mathbf{k}})(a_{\mathbf{k}}^\dagger + a_{-\mathbf{k}}), \end{aligned} \tag{29}$$

where the squeezing function $\tau_{\mathbf{k}}$ is not the same as the one in the insulating case [Eq. (14)], but is given by

$$\tau_{\mathbf{k}}^2 = \sqrt{1 + 4\eta^2\Delta^2 g^2\xi_{\mathbf{k}}^2/W\omega_{\mathbf{k}}^3}. \tag{30}$$

After a Bogoliubov transformation with use of the generator S_4, defined by

$$S_4 = \frac{1}{2}\sum_{\mathbf{k}}\ln(\theta_{\mathbf{k}})(a_{\mathbf{k}}^\dagger a_{-\mathbf{k}}^\dagger - a_{\mathbf{k}}a_{-\mathbf{k}}), \tag{31}$$

we finally obtain the expression for the Hamiltonian as

$$\begin{aligned} e^{S_4}H^S e^{-S_4} = {} & E_g^S + \sum_{\mathbf{k}}\omega_{\mathbf{k}}\tau_{\mathbf{k}}^2 b_{\mathbf{k}}^\dagger b_{\mathbf{k}} + \sum_{\mathbf{k}} W\theta_{\mathbf{k}}^2 a_{\mathbf{k}}^\dagger a_{\mathbf{k}} \\ & - \sum_{\mathbf{k}}\tilde{g}_{S\mathbf{k}}(b_{\mathbf{k}}^\dagger a_{\mathbf{k}} + a_{\mathbf{k}}^\dagger b_{\mathbf{k}}), \end{aligned} \tag{32}$$

where $\tilde{g}_{S\mathbf{k}} = 2g\eta\Delta\tau_{\mathbf{k}}(1-\xi_{\mathbf{k}})/W\theta_{\mathbf{k}}$ with $\theta_{\mathbf{k}}$ and $\xi_{\mathbf{k}}$ given by

$$\theta^2(\mathbf{k}) = \sqrt{1 - 4\eta^2\Delta^2[g^2\xi_{\mathbf{k}}(2-\xi_{\mathbf{k}})/\omega_{\mathbf{k}} - V_0]/W^3}, \tag{33}$$

$$\xi_{\mathbf{k}} = \omega_{\mathbf{k}}\tau_{\mathbf{k}}^2\big/\left(\omega_{\mathbf{k}}\tau_{\mathbf{k}}^2 + W\theta_{\mathbf{k}}^2\right). \tag{34}$$

Note that the displacement function $\xi_{\mathbf{k}}$ in Eq. (34) is different from the one in the insulating case [Eq. (18)].

By referring to the fact that the structure of the coupling between $a_{\mathbf{k}}$ and $b_{\mathbf{k}}$ in $e^{S_4}H^S e^{-S_4}$ is the same as that in the rotating-wave coupling, we can immediately write the ground state of $e^{S_4}H^S e^{-S_4}$ in the form of $|G_S\rangle = |\{a_{\mathbf{k}}^\dagger a_{\mathbf{k}} = 0\}\rangle|\{b_{\mathbf{k}}^\dagger b_{\mathbf{k}} = 0\}\rangle$ with the corresponding ground-state energy of the superfluid phase as

$$\begin{aligned} E_g^S = {} & \frac{1}{2}N\left(\Delta - 2W - 2V_0 + G_{\mathbf{0}}\sigma_0^2\right) \\ & + \frac{1}{4}\sum_{\mathbf{k}}\omega_{\mathbf{k}}\left(\tau_{\mathbf{k}}^2 + \tau_{\mathbf{k}}^{-2} - 2\right) + \frac{1}{2}\sum_{\mathbf{k}} W\theta_{\mathbf{k}}^2. \end{aligned} \tag{35}$$

Two branches of excitations in the superfluid phase $E_S^{\pm}(\mathbf{k})$ are obtained by diagonalization of $e^{S_4}H^S e^{-S_4}$ as

$$E_S^{\pm}(\mathbf{k}) = \frac{1}{2}\left(W\theta_{\mathbf{k}}^2 + \omega_{\mathbf{k}}\tau_{\mathbf{k}}^2\right) \pm \frac{1}{2}\sqrt{\left(W\theta_{\mathbf{k}}^2 - \omega_{\mathbf{k}}\tau_{\mathbf{k}}^2\right)^2 + 4\tilde{g}_{S\mathbf{k}}^2}. \tag{36}$$

Obviously, the following condition must be satisfied for $E_S^-(\mathbf{k})$ to be a stable excitation mode:

$$W\theta_{\mathbf{0}}^2\omega_{\mathbf{0}}\tau_{\mathbf{0}}^2 \geqslant \tilde{g}_{S\mathbf{0}}^2 \Rightarrow 2G_0 \geqslant \eta\Delta. \tag{37}$$

This condition is exactly the complementation of the condition (21). At the transition point, $E_S^-(\mathbf{k})$ is the same as $E_I^-(\mathbf{k})$ (see Fig. 4). But, for $zJ/g = 0.092$ (>0.088 76), $E_S^-(\mathbf{k})$ has a positive gap as shown in Fig. 4.

The gap in the lower-branch excitation spectrum and the order parameter estimated by $\langle G^H|b_{\mathbf{l}}|G^H\rangle$ are shown in Fig. 6 as a function of the hopping parameter zJ/g, where $|G^H\rangle$ denotes the ground state of the original Hamiltonian H. This

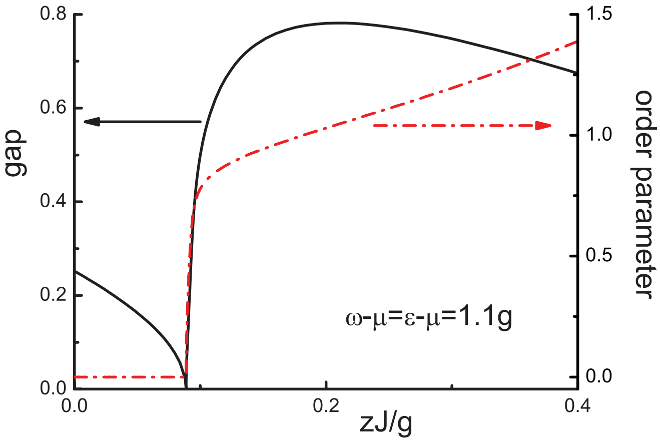

FIG. 6. (Color online) Gap and order parameter as a function of the hopping for the two-dimensional JC square lattice at $\omega = \epsilon$ and $\Delta/g = 1.1$. Energies are in units of ω.

order parameter

$$\langle G^H|b_{\mathbf{l}}|G^H\rangle = \langle G_S|e^{S_4}U^\dagger e^R e^{S_2}e^{S_1}b_{\mathbf{l}}e^{-S_1}e^{-S_2}e^{-R}Ue^{-S_4}|G_S\rangle = \frac{g\sigma_0}{\omega_{\mathbf{0}}} \quad (38)$$

is calculated as the ground-state average of the photonic annihilation operator, and the result is given as $g\sigma_0/\omega_{\mathbf{0}}$. One can see that the gap vanishes at the transition point, and the order parameter grows up from zero for $zJ/g \geqslant 0.088\,76$, indicating a second-order phase transition.

Finally, we add a comment on the gapped excitations from the viewpoint of the Goldstone theorem: For the JC lattice in the RWA, the polariton number $\sum_l(\sigma_l^+\sigma_l^- + b_l^\dagger b_l)$ is conserved, which is similar to the conservation of the total boson number in the Bose-Hubbard model. In the superfluid phase, the emergence of the order parameter $\langle G^H|b_{\mathbf{l}}|G^H\rangle \neq 0$ breaks the number conservation in both models, leading to the Goldstone theorem according to which the gapless bosons should appear to restore the symmetry. When the CRC is included in the JC lattice as in the present case, however, the number conservation is broken from the outset; in this case, we have only the parity conservation with parity operator defined by $\exp[i\pi\sum_l(\sigma_l^+\sigma_l^- + b_l^\dagger b_l)]$, which is a discrete symmetry. Thus, the Goldstone theorem does not apply to our case.

V. CONCLUSION

In summary, we have studied the ground state and the spectra of low-lying excitations of a two-dimensional JC square lattice in both the insulating and the superfluid phases and have shown that, as a result of the competition between the intrasite JC coupling and the intersite photon hopping, a quantum phase transition between the Mott insulator and the long-range superfluid may occur at some critical parameters. The counter-rotating coupling induces a long-range interaction between cavities, which favors the long-range superfluid ordering. The coupling breaks the local conservation of the polariton number, leading to a totally different phase diagram from that in the Bose-Hubbard model. More specifically, the Mott lobes, which are a conspicuous feature in the phase diagram in the Bose-Hubbard model, are totally absent in the JCL.

ACKNOWLEDGMENTS

This work was supported by the National Basic Research Program of China (Grant No. 2011CB922202) and the National Natural Science Foundation of China (Grant No. 10734020). This work was also supported by a Grant-in-Aid for Scientific Research (C) (Grant No. 21540353) as well as Innovative Area "Materials Design through Computics: Complex Correlation and Non-Equilibrium Dynamics" (Grant No. 22104011) from MEXT, Japan.

APPENDIX A: SINGLE-SITE JC MODEL

After the first two unitary transformations with the use of S_1 and S_2, the transformed Hamiltonian H' for the single-site JC model may be written as the sum of three terms H_0', H_1', and H_2', each of which is given as follows:

$$\begin{aligned} H_0' = {} & \frac{1}{2}\epsilon + \frac{1}{2}\eta\epsilon\sigma^z - \frac{g^2}{\omega}\xi(2-\xi) \\ & + \frac{1}{4}\omega\{\tau^2(b^\dagger + b)^2 - \tau^{-2}(b^\dagger - b)^2 - 2\} \\ & - \frac{1}{4}\eta\epsilon\lambda^2(b^\dagger b^\dagger + bb - 2b^\dagger b) - \frac{1}{2}\eta\epsilon(\sigma^z + 1)\lambda^2 b^\dagger b, \end{aligned} \quad (A1)$$

$$H_1' = g\tau(1-\xi)\sigma^x(b^\dagger + b) - \frac{g\eta\epsilon}{\omega\tau}\xi i\sigma^y(b^\dagger - b), \quad (A2)$$

$$\begin{aligned} H_2' = {} & -\frac{\epsilon}{2}\left\{\cosh[\lambda(b^\dagger - b)] - \eta - \eta\frac{\lambda^2}{2}(b^\dagger b^\dagger + bb - 2b^\dagger b)\right\} \\ & - \frac{\epsilon}{2}i\sigma^y\{\sinh[\lambda(b^\dagger - b)] - \eta\lambda(b^\dagger - b)\} \\ & + \frac{\epsilon}{2}(\sigma^z + 1)\{\cosh[\lambda(b^\dagger - b)] - \eta + \eta\lambda^2 b^\dagger b\}, \end{aligned} \quad (A3)$$

where $\lambda = 2g\xi/\omega\tau$ and η is the photon dressing of the level difference, given by $\epsilon\eta = \exp(-\lambda^2/2)$. At this point, no approximation is made and all terms in H' are retained, although some rearrangements among them are made.

By choosing the squeezing parameter τ as

$$\tau^2 = \sqrt{1 + 4\eta\epsilon g^2\xi^2/\omega^3}, \quad (A4)$$

we may diagonalize H_0' into the following form:

$$\begin{aligned} H_0' = {} & E_g + \tfrac{1}{2}\eta\epsilon(1+\sigma^z) + \tfrac{1}{2}\omega(1-\sigma^z)\tau^2 b^\dagger b \\ & + \tfrac{1}{2}\omega(1+\sigma^z)\tau^{-2}b^\dagger b, \end{aligned} \quad (A5)$$

where the constant energy E_g is defined as

$$E_g = \frac{1}{2}\epsilon(1-\eta) - \frac{g^2}{\omega}\xi(2-\xi) + \frac{1}{4}\omega(\tau^2 + \tau^{-2} - 2). \quad (A6)$$

Similarly, by choosing the displacement parameter ξ as

$$\xi = \frac{\omega\tau^2}{\omega\tau^2 + \eta\epsilon}, \quad (A7)$$

we may eliminate the CR terms in H_1', leading to the expression for H_1' as

$$H_1' = \eta\epsilon\lambda(b^\dagger\sigma^- + \sigma^+ b), \quad (A8)$$

in which only the RW terms are present.

An eigenstate of H_0' in Eq. (A5) is described in a form of the direct product $|\pm\rangle|i\rangle$, where $|\pm\rangle$ is the eigenstate of σ_z: $|+\rangle = \binom{1}{0}$ or $|-\rangle = \binom{0}{1}$, and $|i\rangle$ is the photonic number state with i phonons. Then, it is easy to check that the ground state of $H_0' + H_1'$ is described by $|G_1\rangle = |-\rangle|0\rangle$ with the ground-state energy E_g in Eq. (A6), namely,

$$(H_0' + H_1')|G_1\rangle = E_g|G_1\rangle. \tag{A9}$$

With this state $|G_1\rangle$, the ground-state-average polariton number n is given by

$$\begin{aligned} n &= \langle G_1|e^{S_2}e^{S_1}(\sigma^+\sigma^- + b^\dagger b)e^{-S_1}e^{-S_2}|G_1\rangle \\ &= 1 - \eta + \frac{1}{4}(\tau^2 + \tau^{-2} - 2) + \frac{g^2}{\omega^2}\xi^2. \end{aligned} \tag{A10}$$

The results in Eqs. (A6) and (A10) are used in plotting Fig. 1.

Let us examine the effects of H_2' on this state $|G_1\rangle$. The photon operators in H_2' may be expanded as

$$\begin{aligned} &\cosh[\lambda(b^\dagger - b)] - \eta - \eta\frac{\lambda^2}{2}(b^\dagger b^\dagger + bb - 2b^\dagger b) \\ &= \frac{1}{2}\eta[\exp(\lambda b^\dagger)\exp(-\lambda b) + \exp(-\lambda b^\dagger)\exp(\lambda b) \\ &\quad -2 - \lambda^2(b^\dagger b^\dagger + bb - 2b^\dagger b)] = O(\lambda^4), \end{aligned} \tag{A11}$$

$$\begin{aligned} &\sinh[\lambda(b^\dagger - b)] - \eta\lambda(b^\dagger - b) \\ &= \frac{1}{2}\eta[\exp(\lambda b^\dagger)\exp(-\lambda b) - \exp(-\lambda b^\dagger)\exp(\lambda b) \\ &\quad - 2\lambda(b^\dagger - b)] = O(\lambda^3). \end{aligned} \tag{A12}$$

Here, all photon operators are arranged in normal ordering and the renormalization factor η arises from the relation $\exp[\lambda(b^\dagger - b)] = \eta\exp(\lambda b^\dagger)\exp(-\lambda b)$. The results in Eqs. (A11) and (A12) indicate that all zeroth-, first-, and second-order terms of λ are removed from H_2' and, instead, they are put into H_0' and H_1'. Thus, the effects of H_2' on the ground-state energy appear through multiphoton nondiagonal virtual transitions from $|G_1\rangle$.

With this recognition, the correction to E_g due to H_2' may be estimated by perturbation theory with the formula $\Delta E_g = \sum_m |\langle m|H_2'|G_1\rangle|^2/(E_g - E_m)$, where $|m\rangle$ is an excited state of H_0' with energy E_m. Concretely, the correction from the first term in H_2' is given by [see Eq. (A11)]

$$\begin{aligned} C_1 &= -\frac{\eta^2\epsilon^2}{4\omega\tau^2}\sum_{j=2}^{\infty}\frac{(\lambda^2)^{2j}}{2j(2j)!} \\ &= -\frac{\eta^2\epsilon^2}{4\omega\tau^2}\left[\int_0^{\lambda^2}\frac{\cosh(x) - 1}{x}dx - \frac{\lambda^4}{4}\right]. \end{aligned} \tag{A13}$$

Similarly, the correction from the second term in H_2' is less than the quantity C_2, given by [see Eq. (A12)]

$$\begin{aligned} C_2 &= -\frac{\eta^2\epsilon^2}{4\omega\tau^{-2}}\sum_{j=1}^{\infty}\frac{(\lambda^2)^{2j+1}}{(2j+1)(2j+1)!} \\ &= -\frac{\eta^2\epsilon^2}{4\omega\tau^{-2}}\left[\int_0^{\lambda^2}\frac{\sinh(x)}{x}dx - \lambda^2\right]. \end{aligned} \tag{A14}$$

We have estimated the values of C_1 and C_2 for the resonant case with moderately strong coupling ($\omega = \epsilon = g = 1$) to find that $E_g(\text{exact}) = -1.1479$ (numerical exact diagonalization), $E_g(\text{our scheme}) = -1.1330$ [Eq. (A6)], $C_1 = -0.0027$, and $C_2 = -0.0183$, implying that the perturbation correction from H_2' is less than 2%. Thus, we believe that for calculating the ground-state properties, the contribution from H_2' may be safely dropped.

APPENDIX B: DOUBLE-SITE JC MODEL

Calculations for the double-site JC model can be done by extending those for the single-site JC model. A complication arises from the existence of two kinds of photons: in-phase photon with $k = 0, \omega_0 = \omega - J$ and antiphase photon with $k = \pi, \omega_\pi = \omega + J$. After the first two transformations with the use of S_1 and S_2, the transformed Hamiltonian H' containing all terms may be written as the sum of three terms H_0', H_1', and H_2', each of which is given as follows:

$$\begin{aligned} H_0' &= \epsilon - \frac{g^2}{\omega_0}\xi_0(2 - \xi_0) - \frac{g^2}{\omega_\pi}\xi_\pi(2 - \xi_\pi) + \frac{1}{2}\eta\epsilon\left(\sigma_1^z + \sigma_2^z\right) - V\sigma_1^x\sigma_2^x + \frac{\omega_0}{4}\left\{\tau_0^2(b_0^\dagger + b_0)^2 - \tau_0^{-2}(b_0^\dagger - b_0)^2 - 2\right\} \\ &\quad + \frac{\omega_\pi}{4}\left\{\tau_\pi^2(b_\pi^\dagger + b_\pi)^2 - \tau_\pi^{-2}(b_\pi^\dagger - b_\pi)^2 - 2\right\} + \frac{1}{2}\eta\epsilon\left(\sigma_1^z + \sigma_2^z\right)\left\{\lambda_0^2(b_0^\dagger b_0^\dagger + b_0 b_0 - 2b_0^\dagger b_0) + \lambda_\pi^2(b_\pi^\dagger b_\pi^\dagger + b_\pi b_\pi - 2b_\pi^\dagger b_\pi)\right\}, \end{aligned} \tag{B1}$$

$$\begin{aligned} H_1' &= \frac{g}{\sqrt{2}}\tau_0(1 - \xi_0)(b_0^\dagger + b_0)\left(\sigma_1^x + \sigma_2^x\right) - \frac{\eta\epsilon}{\sqrt{2}}\lambda_0(b_0^\dagger - b_0)\left(i\sigma_1^y + i\sigma_2^y\right) \\ &\quad + \frac{g}{\sqrt{2}}\tau_\pi(1 - \xi_\pi)(b_\pi^\dagger + b_\pi)\left(\sigma_1^x - \sigma_2^x\right) - \frac{\eta\epsilon}{\sqrt{2}}\lambda_\pi(b_\pi^\dagger - b_\pi)\left(i\sigma_1^y - i\sigma_2^y\right), \end{aligned} \tag{B2}$$

$$H_2' = -\frac{\epsilon}{2}\sum_{l=1}^{2} i\sigma_l^y[\sinh(X_l) - \eta X_l] \tag{B3}$$

$$+\frac{\epsilon}{2}\sum_{l=1}^{2}\sigma_l^z\left\{\cosh(X_l) - \eta - \eta\lambda_0^2(b_0^\dagger b_0^\dagger + b_0 b_0 - 2b_0^\dagger b_0) - \eta\lambda_\pi^2(b_\pi^\dagger b_\pi^\dagger + b_\pi b_\pi - 2b_\pi^\dagger b_\pi)\right\}, \tag{B4}$$

where the operator X_l and the parameter V are, respectively, introduced as

$$X_l = \sqrt{2}\lambda_0(b_0^\dagger - b_0) - \sqrt{2}(-1)^l\lambda_\pi(b_\pi^\dagger - b_\pi), \quad \text{(B5)}$$

$$V = \frac{g^2}{\omega_0}\xi_0(2-\xi_0) - \frac{g^2}{\omega_\pi}\xi_\pi(2-\xi_\pi), \quad \text{(B6)}$$

with $\lambda_0 = g\xi_0/\omega_0\tau_0$, $\lambda_\pi = g\xi_\pi/\omega_\pi\tau_\pi$, and $\eta = \exp(-\lambda_0^2 - \lambda_\pi^2)$.

The ground state of H_0', $|G_2\rangle$ is represented by the sum of two direct products:

$$|G_2\rangle = (u|-,-\rangle + v|+,+\rangle)|0_0,0_\pi\rangle, \quad \text{(B7)}$$

where $|-,-\rangle$ is the state for both spins in the "−" state, $|0_0,0_\pi\rangle$ is the vacuum state for both in-phase and antiphase photons, the squeezing parameters τ_0 and τ_π are given by

$$\tau_0^2 = \sqrt{1 + \frac{4\eta^2\epsilon^2 g^2\xi_0^2}{Y\omega_0^3}}, \quad \tau_\pi^2 = \sqrt{1 + \frac{4\eta^2\epsilon^2 g^2\xi_\pi^2}{Y\omega_\pi^3}}, \quad \text{(B8)}$$

and the parameters u and v are given as $u = \sqrt{(1+\eta\epsilon/Y)/2}$ and $v = \sqrt{(1-\eta\epsilon/Y)/2}$, respectively, with $Y = \sqrt{\eta^2\epsilon^2 + V^2}$.

The corresponding ground-state energy E_g is obtained as

$$E_g = \epsilon - \sqrt{\eta^2\epsilon^2 + V^2} - \frac{g^2}{\omega_0}\xi_0(2-\xi_0) - \frac{g^2}{\omega_\pi}\xi_\pi(2-\xi_\pi) + \frac{1}{4}\omega_0\left(\tau_0^2 + \tau_0^{-2} - 2\right) + \frac{1}{4}\omega_\pi\left(\tau_\pi^2 + \tau_\pi^{-2} - 2\right). \quad \text{(B9)}$$

By choosing the displacement parameters ξ_0 and ξ_π as

$$\xi_0 = \frac{\omega_0\tau_0^2}{\omega_0\tau_0^2 + Y - V}, \quad \xi_\pi = \frac{\omega_\pi\tau_\pi^2}{\omega_\pi\tau_\pi^2 + Y + V}, \quad \text{(B10)}$$

we can eliminate the CR terms in H_1' to give $H_1'|G_2\rangle = 0$. Finally, the ground-state-average polariton number per site n for the two-site JC model is calculated as

$$\begin{aligned} 2n &= \langle G_2|e^{S_2}e^{S_1}\sum_{l=1,2}(\sigma_l^+\sigma_l^- + b_l^\dagger b_l)e^{-S_1}e^{-S_2}|G_2\rangle \\ &= 1 - \eta^2\epsilon/Y + \sum_{k=0,\pi}\left(\tau_k^2 + \tau_k^{-2} - 2\right)/4 \\ &\quad + \sum_{k=0,\pi} g^2\xi_k^2/\omega_k^2 + g^2V\left(\xi_0^2/\omega_0^2 - \xi_\pi^2/\omega_\pi^2\right)/Y. \end{aligned} \quad \text{(B11)}$$

The results in Eqs. (B9) and (B11) are used in plotting Figs. 2 and 3 .

[1] M. J. Hartmann, F. G. S. L. Brandao, and M. B. Plenio, Laser Photonics Rev. **2**, 527 (2008).
[2] E. Jaynes and F. Cummings, Proc. IEEE **51**, 89 (1963).
[3] A. D. Greentree *et al.*, Nat. Phys. **2**, 856 (2006).
[4] J. Koch and K. Le Hur, Phys. Rev. A **80**, 023811 (2009).
[5] M. P. A. Fisher, P. B. Weichman, G. Grinstein, and D. S. Fisher, Phys. Rev. B **40**, 546 (1989).
[6] M. I. Makin, J. H. Cole, C. Tahan, L. C. L. Hollenberg, and A. D. Greentree, Phys. Rev. A **77**, 053819 (2008).
[7] P. Pippan, H. G. Evertz, and M. Hohenadler, Phys. Rev. A **80**, 033612 (2009).
[8] D. Rossini and R. Fazio, Phys. Rev. Lett. **99**, 186401 (2007).
[9] M. Aichhorn, M. Hohenadler, C. Tahan, and P. B. Littlewood, Phys. Rev. Lett. **100**, 216401 (2008).
[10] M. Knap, E. Arrigoni, and W. von der Linden, Phys. Rev. B **81**, 104303 (2010).
[11] S. Schmidt and G. Blatter, Phys. Rev. Lett. **103**, 086403 (2009); **104**, 216402 (2010).
[12] H. Zheng, S. Y. Zhu, and M. S. Zubairy, Phys. Rev. Lett. **101**, 200404 (2008).
[13] M. O. Scully and M. S. Zubairy, *Quantum Optics* (Cambridge University Press, Cambridge, UK, 1997).
[14] D. C. Mattis, *The Theory of Magnetism* (Springer, Berlin, 1988).